Hindawi
Material Design & Processing Communications
Volume 2023, Article ID 1795150, 9 pages
https://doi.org/10.1155/2023/1795150

Research Article

Investigation of the Effect of Tool Temperature on Microstructure, Hardness, and Wear Behaviour of Aluminium 6061-T6 Alloy Welded by the Friction Stir Welding Process

Mothibeli Pita

Department of Mechanical Engineering, Faculty of Engineering and Technology, University of South Africa, Johannesburg, South Africa

Correspondence should be addressed to Mothibeli Pita; pitam@unisa.ac.za

Received 23 February 2023; Revised 30 March 2023; Accepted 3 May 2023; Published 13 May 2023

Academic Editor: Andrea Tridello

The friction stir welding (FSW) tool is a critical component to the success of the welding process. The aim of the paper is to investigate the effect of tool temperature on the microstructure and mechanical properties of the aluminium alloy during the friction stir welding process. The welding experiment was conducted at a tool rotational speed of 550 rpm, and tool temperature was measured with the increment of a 60 mm distance. Three different tool temperatures were obtained, and samples were characterised by scanning electron microscopy (SEM). The ASTM E384 standard was followed when conducting the Vickers hardness test, and material wear behaviour was tested using the ASTM G99 tribology testing standard. The results show that the tool temperature increases with distance during the FSW process (40.5, 46, and 54°C). A high tool temperature produces the weld butt with high mechanical properties (87.5 HV). The wear rate is low at a high tool temperature ($1.169E-006\ mm^3/N/m$).

1. Introduction

The characteristics of aluminium alloys, such as their low weight, corrosion resistance, specific strength, high formability, and recycling efficiency, make them an appropriate material among other lightweight materials [1]. Despite being more expensive than steel, aluminium alloys 5XXX and 6XXX are the most promising light materials (LM) and are frequently utilized to replace standard steels in vehicle components [2]. Numerous welding techniques can be used to join a variety of materials, including friction stir welding (FSW), friction stir spot welding (FSSW), ultrasonic welding (USW), tungsten inert gas (TIG), laser beam welding (LBW), metal inert gas (MIG), metal active gas (MAG), and arc stud welding (ASW). All of these techniques have various benefits and drawbacks in terms of price, suitability, labour, education, effectiveness, timing, temperature, and simplicity [3]. Friction stir welding (FSW) has drawn considerable interest from many in a variety of industries, including the automotive sector for combining steel and aluminium alloys [4]. The Welding Institute (TWI), in the United Kingdom, developed the friction stir welding (FSW) procedure in 1991, which was regarded as the most important advancement in metal joining in a decade. Despite the fact that it was initially created to combine alloys with aluminium [5], according to recent research, this approach also offers numerous opportunities for the production of light-alloy-based metal-ceramic composites, the joining of incompatible alloys, and surface modification [6]. The FSW technique is a highly reproducible joining method that is successfully employed in a number of high-tech industries, including the automobile, railroad, aerospace, and aviation sectors [7].

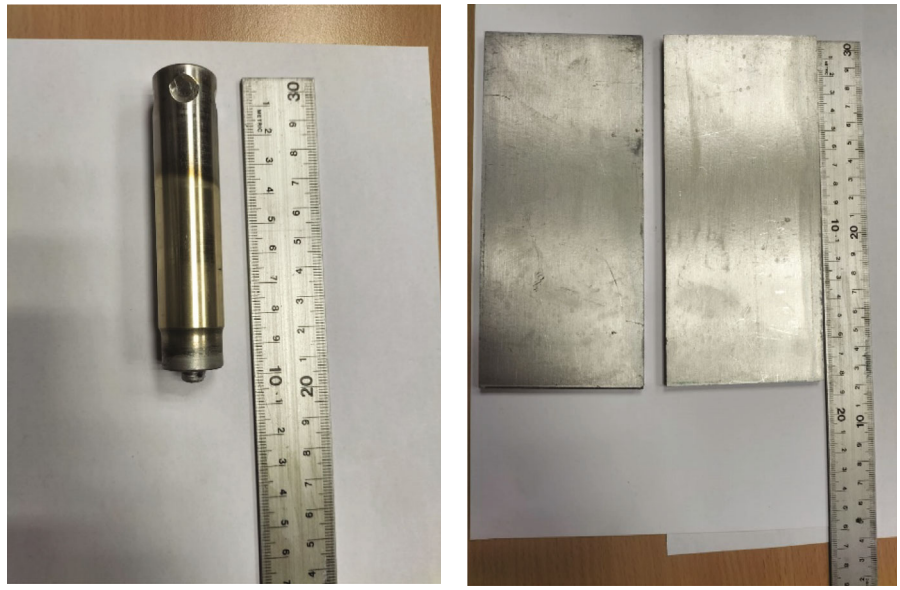

(a) (b)

Figure 1: (a) Material used. (b) Welding tool.

In a FSW process, it is anticipated that the temperature will rise until it is almost at the melting point of the material. However, compared to metals, polymers behave differently throughout the welding process [8]. Heat is produced, the material becomes softer, and plastic deformation is made possible by the friction between the tool and the workpiece [9]. The FSW tool has a profiled pin and is cylindrical in shape. It typically touches the component while welding [10]. Numerous investigations on the impact of friction stir welding temperature have been done. In 2015, the study of the effect of the friction stir welding tool on temperature, applied forces, and weld quality was conducted by [11]. It was found that the generated temperature, axial and translational stresses, and weld properties were all directly connected with the tool shoulder diameter. An analysis of temperature distribution and mechanical properties of friction stir welding of Al-Cu joints using hardened H13 steel tools was carried out. High ultimate tensile strength and impact strength were discovered to be produced at 1200 rpm tool rotational speed and 20 mm/min feed rate with the square pin profile of a hardened H13 steel tool due to the highest temperature at weld areas [12]. It has been observed that frictional temperature increases greatly when rotating speed and tilt angle increase, but adversely as welding speed increases. This was observed during a study on the friction stir welding of armour-grade aluminium alloy and the effects of process parameters on temperature and force distribution [13].

Industrial tribology is an emerging field [14]. The consequences of friction and wear are many. Friction and wear typically result in material and energy loss, as well as costs to the social system that uses the mechanical equipment [15]. The ideas of wear, lubrication, and friction are all included in tribology. According to several academics, this area of technology is intimately related to mechanical engineering and materials science [16]. In addition to overhaul and machine turnover, the UK industry survey in 1997 estimated the cost of wear to be roughly £650 million [17]. The principles of tribology must be understood in the design of tools, gears, machines, and other engineering applications [18].

Due to the friction stir welding technique's high heat production, the temperature of both the material being welded and the tool being utilized increases. The complicated nature of the heat produced by this welding process has a significant impact on the finished parts' quality [19]. During the FSW process, temperature generation and its distribution over various regions have a stimulating effect on the microstructural characteristics and mechanical characteristics of the manufactured welds [20]. It is imperative to investigate the effect of tool temperature on the microstructure and mechanical properties of a sample welded by friction stir welding. The tool temperature will be measured using a noncontact infrared thermometer at intervals of 60 mm distance. This method is cost-effective, quick, and easy to perform.

2. Material

Aluminium alloy 6061-T6 material of 180 mm long × 75 mm wide and 6 mm thick was used in this study. A cylindrical welding tool of 20 mm in diameter with a conical threaded pin 5 mm in diameter and 5 mm in length was used to join the two materials. Both material and the tool used in this study are shown in Figure 1.

3. Chemical Composition

ESD was conducted on a welded sample, and it was found that the material is pure aluminium as illustrated in Figure 2.

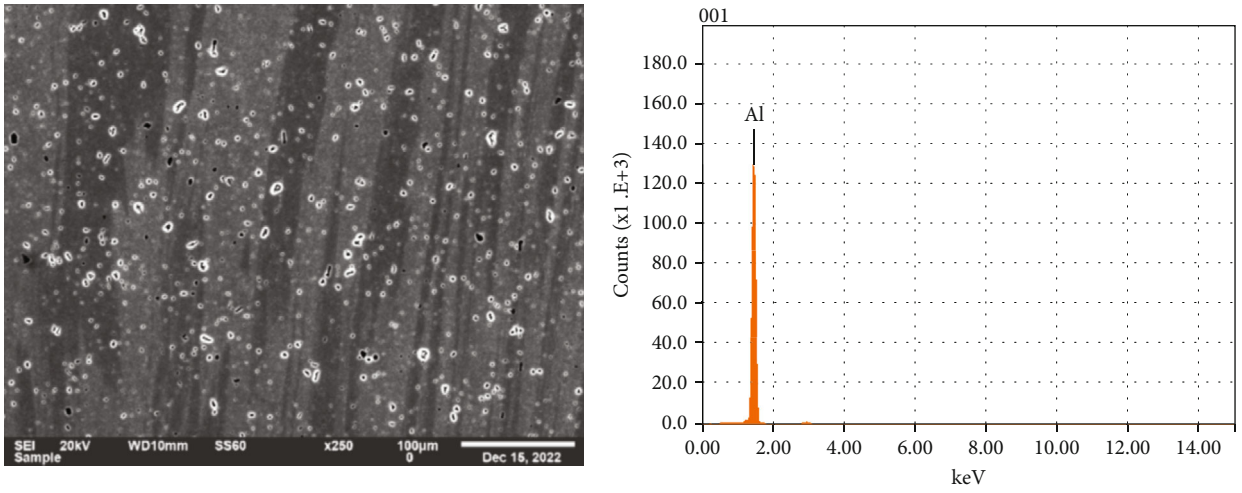

(a) (b)

Figure 2: EDS spectrum.

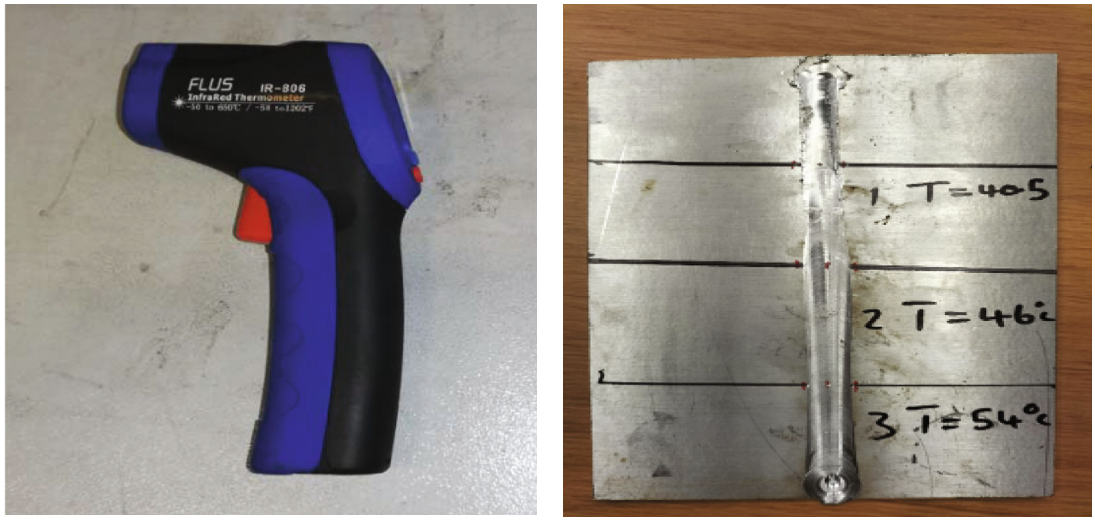

(a) (b)

Figure 3: (a) Infrared thermometer. (b) Welded sample sectioned according to tool temperature.

4. Friction Stir Welding Experimentation

In this study, a continuous friction stir welding process was used to join two aluminium alloy 6061-T6 materials of 180 mm long, 75 mm wide, and 6 mm thick. The tool temperature was measured before the welding process and recorded using a noncontact infrared thermometer (FLUS IR-806), ranging from -50 to 650°C which is presented in Figure 3(a). The tool temperature was also measured during the welding process at intervals of 60 mm throughout the process, and it is illustrated in Figure 3(b). The tool temperature and distance rerecorded during the welding process are presented in Table 1. An I-STIR PaR system technology friction welding machine was used to weld the aluminium material, and it is shown in Figure 4(a). The samples to be welded were clamped at six different positions to ensure that they do not separate during the welding process, as shown in Figure 4(b) [21]. Welding parameters were used in this study. The samples were welded at a tool rotational speed of 550 rpm and a feed rate of 300 mm/min, with a depth of 3.5 mm and a forging force of 1 kN.

Table 1: Tool temperature and distance travelled.

Tool temperature (°C)	Distance (mm)
19.3	0
40.5	60
46	120
54	180

5. Sample Preparation and Characterisation

Cross-sections of the metallographic samples were taken in the rolling direction. The samples were cold-mounted in

(a) (b)

Figure 4: (a) I-STIR PaR system technology FWS machine and (b) material clamping.

plastic resin made of ClaroCit. By following the ASTM E3-01 metallographic sample preparation standard, the mounts were fine ground with #220, #800, and #1200 grit SiC papers and then plane ground with #120 grit SiC paper. Using diamond lubricants in polishing phases of 9 m, 6 m, and 1 m on magnetic discs, the mounts were polished to a mirror surface finish by Mol and Nap cloths. After that, Barker's reagent was used to electrolytically etch the mounts. Using a Struers LectroPol-5 electropolishing and etching machine, electroetching was carried out for 4 minutes using a 1.8% HBF6 electrolyte solution, while the machine was adjusted to 30 volts dc, a flow rate of 15 ml/min, and a current density of 5 A/cm^2. The sample surface was cleaned under running water, and then, compressed air was used to dry it. Under an optical light microscope, the mounts were inspected and photographed (Olympus DSX50). Using a scanning electron microscope, 250x magnification was used to create the macrographs.

5.1. Microhardness Test. Welded samples were cut, mounted, ground, and polished before microhardness tests. A Vickers (HV 10) hardness test was performed on welded samples of three different tool temperatures according to the ASTM E384 standard and is presented in Table 2. EMCO-TEST hardness test machine was used. Three indentations were made per sample for statistical considerations.

5.2. Tribology Test. Welded samples that were cut, mounted, and polished underwent dry tribology tests. The tribology testing standard ASTM G99 was used. The samples were tested after being welded at various tool temperatures to determine the coefficient of friction and wear rate. Figure 5 shows how the samples' wear behaviour was evaluated at room temperature using an Anton Paar TRB3 pin-on-disk tribometer. A steel counterface ball was utilized in dry conditions with a force of 15 N, a radius of 0.39 mm, and an

Table 2: Material hardness and different tool temperatures.

Tool temperature	T_1 (40.5°C)	T_2 (46°C)	T_3 (54°C)
Test 1	63 HV	77.4	91.3
Test 2	72.4 HV	78.3	89.1
Test 3	75.7 HV	70.9	82.1
Mean	70.4 HV	75.5 HV	87.5 HV
Standard deviation	6.6	4.0	4.8
Error bars	3.8	2.3	2.8

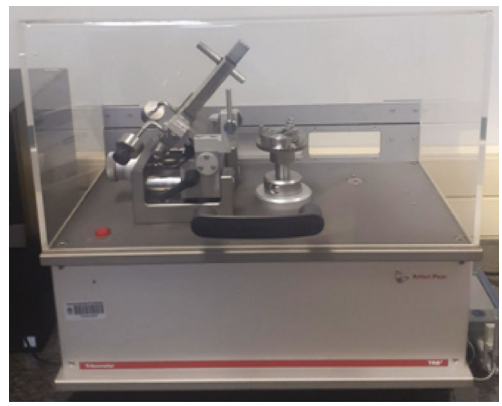

Figure 5: Anton Paar's tribometer machine [18].

Table 3: Tribology test results.

Sample	Coefficient of friction	Wear rate (mm^3/N/m)
T_1	0.277	0.0006304
T_2	0.305	$4.82E-005$
T_3	0.311	$1.169E-006$

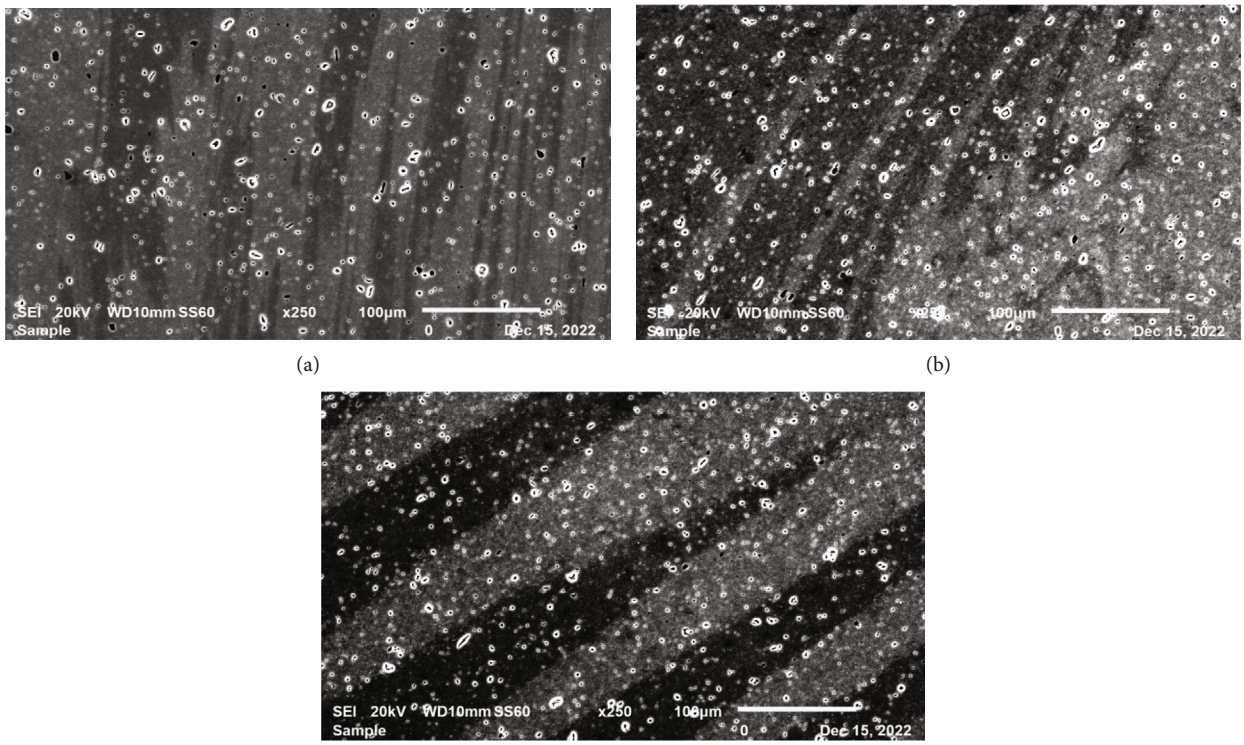

Figure 6: SEM micrographs of (a) 60 mm distance, (b) 120 mm distance, and (c) 180 mm distance.

acquisition rate of 80 Hz against the samples. These tests were conducted at a room temperature of 25.65°C using a 6 mm ball shape. The outcomes of wear rate testing were noted and are shown in Table 3.

6. Results and Discussions

A continuous friction stir welding process was conducted in this study. However, tool temperature was measured before and during the welding process using an infrared thermometer, and the results are recorded in Table 1. Before commencing with the welding process, the tool temperature was measured and recorded as 19.3°C. The welding process was started, and at the 60 mm distance from the starting point, the tool temperature increased by 52.3%. The tool temperature continued to increase until it reached 54°C, which was at a distance of 180 mm. In this welding process, friction is created between the tool and material, which results in heat generation. The process needs to create a lot of heat which will plasticise the two materials to be joined. Inadequate heat during this welding process will result in poor adhesion, and there will be welding defects.

7. Microstructure Studies

The microstructure of the friction-stir-welded aluminium alloy joint is illustrated in Figures 6(a)–6(c). Characterisation was done on a weld zone using scanning electron microscopy. From these three figures, the tool tracks were visible. They were more visible at the joints made of 54°C tool temperature. At this distance (180 mm), the materials were more plasticised due to higher heat content at this point. In Figures 6(a)–6(c), scattered welding porosity has been observed, which is normally linked to welding operations, welding conditions, and faulty consumables. ImageJ was used to measure the size of porosity on the samples, and this was graphically shown in Figures 7(a)–7(c). Porosity is the contaminant or gas absorbed into the weld puddle. The results reveal the biggest size at a lower tool temperature, which was 3.3 μm. Similar results were obtained by [22]. The porosity sizes of tool temperatures of 46 and 54°C were almost the same and reported to be 1.8 and 1.83 μm, respectively. This is the welding flaw that develops as a result of unwelcome gasses being trapped during the solidification of the molten weld puddle. According to a report, hydrogen porosity can be efficiently decreased by speeding up the welding process so that there is not enough time for the hydrogen to build up due to the quick cooling and solidification [23]. Figure 7(a) shows the high frequency discovered on 1 and 2 μm, while in Figure 7(b), it was in a diameter between 1 and 1.5 μm.

7.1. Hardness Test Results. The microwelding hardness of three samples was tested and is graphically illustrated in Figure 8. This method was used to measure the average hardness in order to estimate the mechanical properties of the weld joint. It was noticed that at a high tool temperature (54°C), the weld becomes the hardest (87.5 HV), and it becomes softer (70.4 HV) at lower tool temperatures

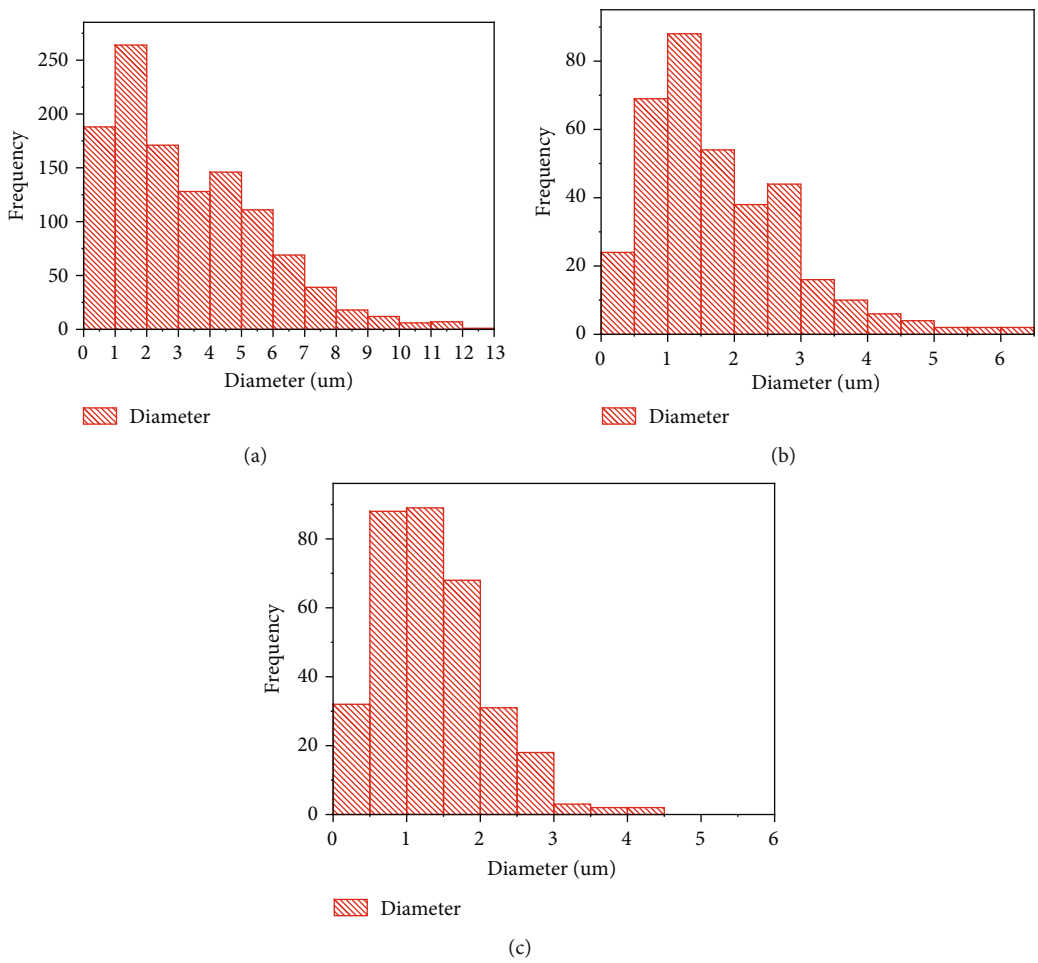

Figure 7: Porosity size (a) tool temperature of 40.5°C, (b) tool temperature of 46°C, and (c) tool temperature of 54°C.

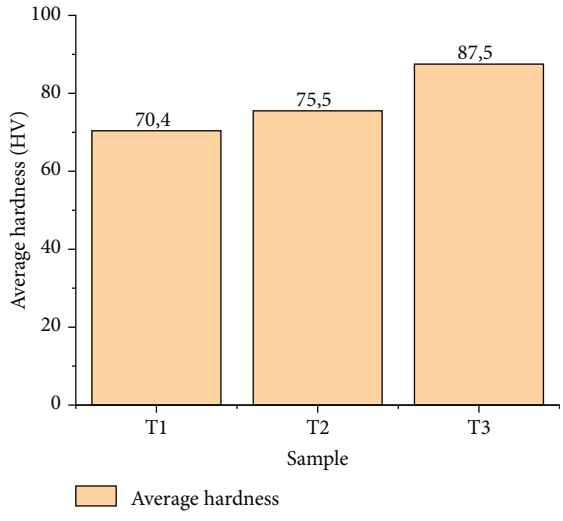

Figure 8: Average hardness at different tool temperatures.

(40.5°C). According to reports, increasing the process temperature causes the overaged precipitates to dissolve more effectively, increasing the hardness as a result since the precipitates are distributed evenly [24]. It shows that the high tool temperature plasticises the material and makes the two pieces bond properly. When the tool's traverse and rotating speed both increase at the same time, the welded joints' mechanical strength rises [25].

7.2. Tribology Test Results. A tribology test was conducted on a welded sample at a force of 15 N and linear speed of 0.08 cm/s. This test was performed to measure the amount of friction that exists between the welded surface and the steel ball of 10 mm diameter. Table 3 presents the results obtained during the tribology test which is graphically illustrated in Figures 9 and 10. It was noticed in Figure 9(a) that less force is required for sliding to occur on a weld made by a tool temperature of 40.5°C because it was reported to have the lowest coefficient of friction (0.277). At a high tool temperature (54°C), which is presented in Figure 9(c), it was observed that more force is required for sliding to occur as it was reported to have the highest coefficient of friction (0.311). Figure 10 reveals that the wear rate was high at the welding joint made by a lower tool temperature, which was reported to be 0.0006304 mm^3/N/m. The wear rate was lower at the highest tool temperature (54°C) and was recorded as $1.169E-006$.

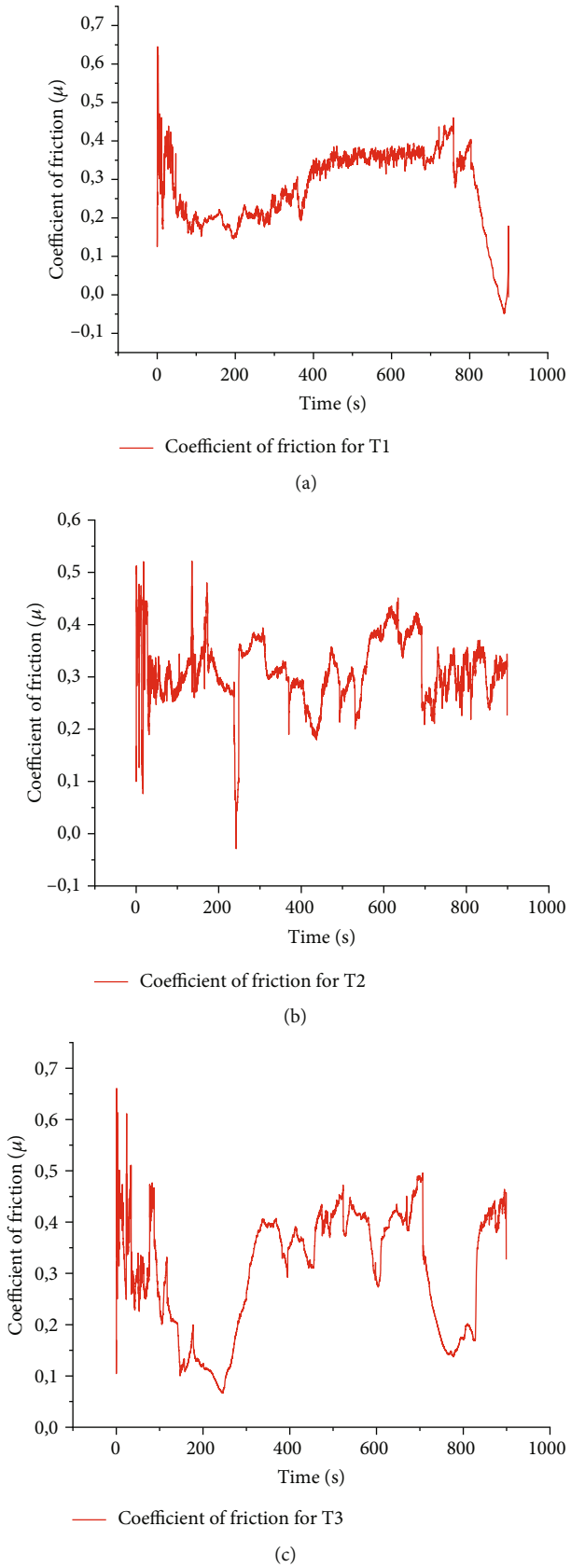

Figure 9: Coefficient of friction (a) tool temperature of 40.5°C, (b) tool temperature of 46°C, and (c) tool temperature of 54°C.

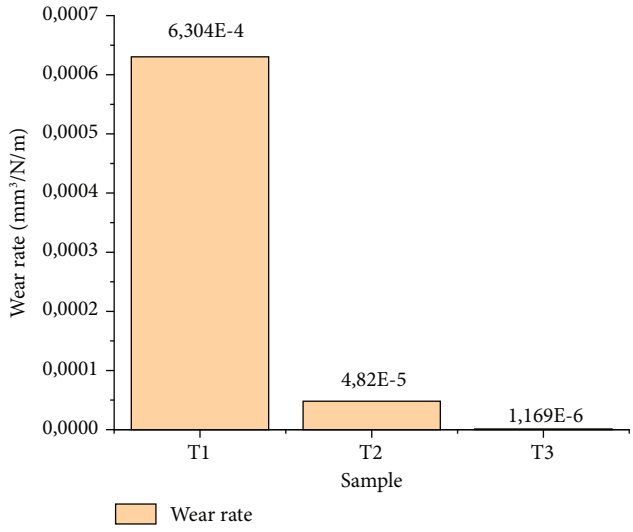

Figure 10: Wear behaviour per tool temperature.

8. Conclusion

In this research paper, the effect of tool temperature on microstructure, hardness, and wear behaviour of aluminium 6061-T6 alloy weld joints was investigated. It was noted that during the friction stir welding process, the tool temperature increases (from 19.3°C to 40.5°C and 46°C to 54°C) with respect to welding distance (from 0 with intervals of 60 mm), which generates more heat on the material being welded. Welding defects were found on all welded samples, which result from unwanted gasses being trapped within the molten weld puddle during solidification. The high tool temperature (54°C) produces the weld joint with high mechanical properties (87.5 HV). The coefficient of friction is high (0.311) at a high welding temperature. The welding joint wears faster at low tool temperature (40.3°C), and the wear rate was low ($1.169E-006$) when the welding temperature is high (54°C). It can be concluded that inadequate heat during the friction stir welding process will result in poor adhesion, and there will be welding defects. More heat is required during the FSW process to plasticise the material which will increase the bond of the two materials being welded. By doing so, a joint with high mechanical properties will be produced.

Data Availability

The data used to support the findings of this study are available from the corresponding author upon request.

Conflicts of Interest

The author declares that they have no conflicts of interest.

Acknowledgments

Mr. Gaonnwe is acknowledged for his assistance with the tests. The University of South Africa deserves special recognition for providing the resources and financial assistance necessary to carry out this research. Open Access funding was enabled and organized by SANLiC Gold.

References

[1] Y.-B. Lim and K.-J. Lee, "Microtexture and microstructural evolution of friction stir welded AA5052-H32 joints," *Journal of Welding and Joining*, vol. 37, no. 2, pp. 35–40, 2019.

[2] H.-S. Bang, H.-S. Bang, and K.-H. Kim, "Effects of process parameters on friction stir weldability in dissimilar joints of AA5052 and advanced high strength steel," *Journal of Welding and Joining*, vol. 39, no. 2, pp. 189–197, 2021.

[3] H. R. Ghazvinloo and N. Shadfar, "Effect of friction stir welding parameters on the quality of Al-6% Si aluminum alloy joints," *Journal of Materials and Environmental Science*, vol. 11, no. 5, pp. 751–758, 2020.

[4] A. Alimohamady, A. Eghlimi, H. N. Foroshani, M. A. Behzadi, J. Mohammadi, and M. K. Asgarani, "Friction stir welding of EN 10130 low carbon steel," *Journal of Welding and Joining*, vol. 38, no. 3, pp. 269–277, 2020.

[5] M. Puviyarasan, L. Karthikeyan, C. Gnanavel, and K. Dhineshkumar, "A critical review on friction stir based processes," in *Proceedings of the International Conference for Phoenixes on Emerging Current Trends in Engineering and Management (PECTEAM 2018)*, pp. 258–266, India, February 2018.

[6] R. Kosturek, L. Śnieżek, J. Torzewski, and M. Wachowski, "Research on the friction stir welding of Sc-modified AA2519 extrusion," *Metals*, vol. 9, no. 10, p. 1024, 2019.

[7] W. Muhammad, W. Husain, A. Tauqir, and A. Wadood, "Optimization of friction stir welding parameters of AA2014-T6 alloy using Taguchi statistical approach," *Journal of Welding and Joining*, vol. 38, no. 5, pp. 493–501, 2020.

[8] S. Eslami, T. Ramos, P. J. Tavares, and P. M. G. P. Moreira, "Effect of friction stir welding parameters with newly developed tool for lap joint of dissimilar polymers," *Procedia Engineering*, vol. 114, pp. 199–207, 2015.

[9] A. C. F. Silva, J. De Backer, and G. Bolmsjö, "Temperature measurements during friction stir welding," *International Journal of Advanced Manufacturing Technology*, vol. 88, no. 9–12, pp. 2899–2908, 2017.

[10] P. Jayaseelan, S. Rajesh Ruban, M. Suresh, N. S. Gowtham, and P. Saravanan, "Thermal analysis of pentagonal profiled friction stir welding tool using Ansys," *IOP Conference Series: Materials Science and Engineering*, vol. 993, no. 1, pp. 1–11, 2020.

[11] H. Papahn, P. Bahemmat, M. Haghpanahi, and I. P. Aminaie, "Effect of friction stir welding tool on temperature, applied forces and weld quality," *IET Science, Measurement and Technology*, vol. 9, no. 4, pp. 475–484, 2015.

[12] J. Pratap Kumar, A. Raj, A. R. Venkatraman et al., "Analysis of temperature distribution and mechanical properties of friction stir welding of Al-Cu joints using hardened H13 steel tools," *Advances in Materials Science and Engineering*, vol. 2022, Article ID 4973839, 14 pages, 2022.

[13] S. Verma and J. P. Misra, "Effect of process parameters on temperature and force distribution during friction stir welding of armor-marine grade aluminum alloy," *Proceedings of the Institution of Mechanical Engineers, Part B: Journal of Engineering Manufacture*, vol. 235, no. 1–2, pp. 144–154, 2021.

[14] A. Hussain, V. Podgursky, D. Goljandin, M. Antonov, M. A. Basit, and T. Ahmad, "Mild steel tribology for circular economy of textile industries," *Tribology in Industry*, vol. 43, no. 4, pp. 552–560, 2021.

[15] R. C. Singh, M. S. Ranganath, and G. Shukla, "Tribological analysis of etched mild steel surface," in *International conference of advance research and innovation*, pp. 296–304, China, 2015.

[16] A. Shalwan, B. F. Yousif, F. H. Alajmi, K. R. Alrashdan, and M. Alajmi, "Tribological investigation of frictional behaviour of mild steel under canola bio-lubricant conditions," *Tribology in Industry*, vol. 42, no. 3, pp. 481–493, 2020.

[17] A. Milanti, H. Koivuluoto, P. Vuoristo, G. Bolelli, F. Bozza, and L. Lusvarghi, "Microstructural characteristics and tribological behavior of HVOF-sprayed novel Fe-based alloy coatings," *Coatings*, vol. 4, no. 1, pp. 98–120, 2014.

[18] M. Pita and L. Lebea, "Investigating the effect of cooling media on hardness, toughness, coefficient of friction, and wear rate of mild steel heat treated at different temperatures," *Material Design & Processing Communications*, vol. 2022, article 3564875, 10 pages, 2022.

[19] S. D. Dhanesh Babu, P. Sevvel, R. Senthil Kumar, V. Vijayan, and J. Subramani, "Development of thermo mechanical model for prediction of temperature diffusion in different FSW tool pin geometries during joining of AZ80A Mg alloys," *Journal of Inorganic and Organometallic Polymers and Materials*, vol. 31, no. 7, pp. 3196–3212, 2021.

[20] P. Sevvel, S. D. Dhanesh Babu, and R. Senthil Kumar, "Peak temperature correlation and temperature distribution during joining of AZ80A Mg alloy by FSW - a numerical and experimental investigation," *Strojniški vestnik – Journal of Mechanical Engineering*, vol. 66, no. 6, pp. 395–407, 2020.

[21] T. Gaonnwe, M. Mashinini, and M. Pita, "The effect of cold rolling on mechanical properties and microstructure of aluminium 6082 T6 joint by friction stir welding process," *MATEC Web of Conferences*, vol. 370, article 03015, 2022.

[22] Q.-t. Wang, X.-n. Wang, X.-m. Chen et al., "Interactive effects of porosity and microstructure on strength of 6063 aluminum alloy CMT MIX + synchropulse welded joint," *Transactions of Nonferrous Metals Society of China*, vol. 32, no. 3, pp. 801–811, 2022.

[23] P. Kah, R. Rajan, J. Martikainen, and R. Suoranta, "Investigation of weld defects in friction-stir welding and fusion welding of aluminium alloys," *International Journal of Mechanical and Materials Engineering*, vol. 10, no. 1, p. 26, 2015.

[24] S. Suenger, M. Kreissle, M. Kahnert, and M. F. Zaeh, "Influence of process temperature on hardness of friction stir welded high strength aluminum alloys for aerospace applications," *Procedia CIRP*, vol. 24, pp. 120–124, 2014.

[25] C. Satheesh, P. Sevvel, and R. S. Kumar, "Experimental identification of optimized process parameters for fsw of az91c mg alloy using quadratic regression models," *Strojniški vestnik – Journal of Mechanical Engineering*, vol. 66, no. 12, pp. 736–751, 2020.